Title	A Congestion Alleviation Technique Exploiting Structural Insights on the Interaction of Line Loading Limits, Reactance and Line Outage Security Constraints
Authors(s)	Beiranvand, Arash, Cuffe, Paul
Publication date	2022-08-15
Publication information	Beiranvand, Arash, and Paul Cuffe. "A Congestion Alleviation Technique Exploiting Structural Insights on the Interaction of Line Loading Limits, Reactance and Line Outage Security Constraints." IEEE, August 15, 2022. https://doi.org/10.1109/TPWRS.2022.3198487.
Publisher	IEEE
Item record/more information	http://hdl.handle.net/10197/25726
Publisher's version (DOI)	10.1109/TPWRS.2022.3198487
Notes	Referred to by: http://hdl.handle.net/10197/26505; published version: https://doi.org/10.1109/TPWRS.2023.3328203

A Congestion Alleviation Technique Exploiting Structural Insights on the Interaction of Line Loading Limits, Reactance and Line Outage Security Constraints

Arash Beiranvand and Paul Cuffe, *Senior Member, IEEE*

***Abstract*—Line outage security constraints ensure that a proposed generating schedule will not load any line to the point where its removal causes more overloading elsewhere. These security constraints increase operating costs by occasionally precluding the usage of the cheapest generation sources. That is, power networks frequently suffer *congestion* in this $(N-1)$ sense. To explore the structural origins of such $(N-1)$ congestion, this paper defines a new metric for branches within a grid, *shadow capacity*, which gauges the maximum flow on a branch before its removal would tend to overload other lines elsewhere. Using this novel metric, we argue the $(N-1)$ congestion is a consequence of imbalances in the pattern of line reactances and capacities across a network. To further explore the insights offered by the shadow capacity analysis, a novel methodology to relieve $(N-1)$ congestion and hence improve the grid's loadability is developed. This technique adds fixed reactance to certain lines in the grid to boost their shadow capacities. These results show modest alleviation of actual $(N-1)$ congestion, which shows the potential value of optimising power networks through the lens of shadow capacity enhancement.**

NOMENCLATURE

Constants

L_{ij}	Line connecting node i to node j
X_l	Reactance of line l
Λ^{st}	Injected power at bus s and withdrawn at bus t
Z_{bus}	Grid's impedance matrix
Y_{bus}	Grid's admittance matrix
x_{is}	Imaginary part of the component at row i and column s within Z_{bus}
C_l	Thermal capacity of l
X	Fixed extra reactance added to the identified lines
X^0_{ij}	Original natural reactance of L_{ij}
a_k	Status of line k
M_{ij}	A sufficiently big and positive number corresponding to L_{ij}
μ	Percentage of active generators for a particular generation schedule
$\mathcal{G}^0_i$	Generation level for generator i under the initial infeasible dispatch
D_i	Total demand at bus i

Sets and Indices

$\hat{L}$	Set of grid's non-radial lines
L	Set of grid's lines
N	Set of grid's buses
$L^{'}$	Set of grid's lines except k
S_k	Vector of loading levels for line k
$\mathbb{G}$	Set of grid's generators
$\mathbb{G}_i$	Set of the generators connected to bus i
G	Set of notional generators used by the methodology to improve the median shadow capacities

Variables and functions

Π	PTDF matrix
${\Pi_l}^{st}$	Flow change in line l due to the injection of 1 MW at bus s and withdrawal at bus t
$\Delta\delta$	Buses' voltage angles changes matrix
Θ^{st}_l	Power flow change on line l for injecting of Λ MW at bus s and withdrawing it at bus t
ΔP	Nodal power injection matrix
Ψ	LODF matrix
${\Psi_l}^k$	Corresponding component of l within LODF matrix for a line k outage
Φ_k	Median shadow capacity for line k
Δ_k	Loading capacity decrease experienced by line k
$\mathcal{G}_i$	The generator connected to bus i
g_k	Notional generator corresponding to line k
P^k_{ij}	Power flow on L_{ij} for line k outage
δ_i	Voltage angle of bus i
δ_s	Voltage angle of slack bus
$X^{'}_{ij}$	Total reactance of L_{ij}
U_{ij}	Binary decision variable corresponding to L_{ij}
γ^k_{ij}	Continuous variables corresponding to L_{ij} in outage scenario k

LIST OF ABBREVIATIONS

DC-PF	DC Power Flow
DSR	Distributed Series Reactances
MILP	Mixed Integer Linear Programming
LODF	Line Outage Distribution Factors
OPF	Optimal Power Flow
OTS	Optimal Transmission Switching

A. Beiranvand (arash.beiranvand@ucd.ie) and P. Cuffe are with the School of Electrical and Electronic Engineering, University College Dublin. This publication has emanated from research supported in part by Science Foundation Ireland (SFI) under the SFI Strategic Partnership Programme Grant Number SFI/15/SPP/ E3125 and additional funding provided by the UCD Energy Institute. The opinions, findings and conclusions or recommendations expressed in this material are those of the authors and do not necessarily reflect the views of the Science Foundation Ireland.

PTDF Power Transfer Distribution Factor
RES Renewable Energy Sources

I. Introduction

TRANSMISSION network congestion refers to a condition whereby the grid can not facilitate desired power transactions or generation schedules due to operational limitations [1], [2]. We can distinguish two varieties of congestion based on the types of operational limitations encountered: $(N-0)$ and $(N-k)$ related congestion. In the more visible $(N-0)$ sense, the congestion is simply due to the basic limitations of transmission assets *before* any contingencies arise: for instance, where lines' thermal capacities simply cannot accommodate the required power flow (note that longer lines, and those at higher voltages, may often be constrained by voltage stability limits [3] rather than thermal limits: for simplicity, and without loss of generality, the present paper uses the latter as the parameter that characterises a line's maximum permissible loading.)

Congestion in the $(N-k)$ sense refers to network security constraints that become binding for a particular contingency situation. Such $(N-k)$ security constraints potentially precludes the full use of the capacities of all the lines, so that the accidental disconnection of any one line would not cause overloads anywhere else. For instance, $(N-1)$ contingency constraints should guarantee that a power system is secure against the failure of any one element. This $(N-1)$ criteria is fundamental to secure network planning and operation, and is typically mandated by grid standards documents [4].

Imposing these essential $(N-1)$ line outage contingency constraints within the optimal dispatch problem may entail congestion costs [5], as they can restrict the usable capacity of a line and thereby necessitate the scheduling of more costly generators [1], [5]–[7]. For instance, [2] reports congestion costs (including the costs related to the $(N-1)$ reliability criteria) in the range of hundreds of millions of dollars annually to securely operate various American transmission systems. Studies related to improving the loadability of power grids routinely deal with the congestion stemming from imposing $(N-1)$ security constraints and hence, provide congestion management methodologies to address the issue. Typically, these congestion management solutions fall into three main categories: 1) the strategies that contemplate implementing FACTS devices to improve the grid's loadability, 2) the approaches that target the topology of the grid to alleviate congestion, and 3) the studies that address the challenges at the level of the power market.

Concerning implementing FACTS devices to improve the loadability of a power grid, the works in [8]–[12] are some examples of such studies in which the deployment of the devices aims to achieve a more secure loading profile for the grids in terms of the contingencies the network may encounter. The studies related to optimal transmission switching (OTS) are another strand of research that mitigate the congestion stemming from line outages security constraints, including $(N-1)$ security constraints, by deliberately switching out lines to accommodate a particular generation schedules. Various techniques have been proposed in the literature [12]–[19] for the optimal selection of such lines.

Notably, the OTS technique modifies the grid's structure to optimise its loading condition. There are various examples in the literature which seek to link a grid's structural features with the line loading profile and contingency conditions. For example, the authors of [20] analysed the influence of an outage in heavily loaded power flow-gates within a power grid and conclude that such outages could expose the grid to additional outages and even blackouts. Consequently, a novel topological technique based on graph theory was developed in [20] to screen these power flow transactions across the grids. In [21], these authors further developed their topological-based approaches to detect such vulnerabilities connected to a "saturated cut-set" [20] after the removal of a line in a power system. The work in [22], by the present authors, is another example of using the topological specifications of a power grid to investigate its lines' loading redistribution following a contingency where, relying on graph theory, a novel concept termed "coherent cut-set" was defined and used to identify some of the most significant $(N-k)$ contingencies for the grid. Recent instances of exploiting topological characteristics of a power grid to assess its loading capabilities and some of its most significant $(N-k)$ contingencies can be found in [23]–[25].

As previously stated, a third strand of research on the congestion issue studies it at the level of the market. The papers given in [5], [26]–[29] are examples of such an approach. For example, the problem of generation dispatch feasibility provided by the market operator is investigated in [29]. For this purpose, different operation constraints are considered that include but are not limited to: the bus voltage constraints, the line overloading constraints, and $(N-1)$ and $(N-2)$ security constraints. The authors in [5] developed a novel transmission fixed cost allocation model. The proposed model is applicable for a pool-based power market, and the $(N-1)$ security constraints are considered for annual grid operation. For each time interval during a year, all $(N-1)$ contingencies are considered. Then, a security-constrained optimal power flow is solved to determine the maximum power flow the transmission network may experience following each contingency. Here, the maximum loadability of the grid is considered as the optimal capacity of the transmission network. Each facility is then charged for its network usage in the largest grid loadability during the year. In this way, the congestion costs are allocated fairly to the facilities.

In addition to the three primary categories of methodologies used to research power grid congestion, there is a fourth approach that includes curative congestion management strategies to address the issue. For instance, Hoffrichter et al. in [30] opted for a curative congestion management strategy as they believe that a curative management strategy relying on the post-contingency operation condition provides more utilization in pre-contingency. They argue that due to the capabilities of today's power grids, such as operating a variety of FACTS devices and battery storage units, the operators can account for the abilities' of the grid to come up with the contingencies. Therefore, Hoffrichter et al. concluded that opting for curative congestion management seems to be reasonable.

What, though, is the root cause of $(N-1)$ congestion? The present paper argues that $(N-1)$ congestion is a direct consequence of the topological and reactance structure of a power system, and the interaction of these with line capacity ratings. To substantiate this argument, we define a new topological metric for power system lines, termed *median shadow capacity*, which gauges how heavily a particular line can be loaded before its removal would tend to cause overloading on adjacent network elements. This new structural metric brings to light the maximum possible loading capacity of each line for which the $(N-1)$ security constraints can be upheld for the grid. Using this novel metric, bottlenecks can be detected: those particular lines which markedly restrict the loadability of other lines in the grids by inducing congestion in the $(N-1)$ sense.

The median shadow capacity is calculated using the *Line Outage Distribution Factors* (LODF) [31], which quantify how a line's pre-outage power flow will be redistributed onto adjacent lines if it is removed [32]. The LODF matrix derives solely from the connective topology and reactance of the branches comprising a network. This new metric can therefore articulate how a line's reactance, capacity, and location within a meshed network interact with the $(N-1)$ security constraints to cause congestion elsewhere. This leads to the claim that the $(N-1)$ congestion of a power grid is mainly caused by *imbalances* in the reactance structure of the grid and the lines' loading capacities. Discussion and tutorial treatments on this core theoretical point are provided in Section II of this paper.

Building on this idea, a novel strategy for relieving the $(N-1)$ congestion is then proposed. This technique uses insights from the shadow capacity analysis to identify those lines in a grid whose reactance should be *increased* to mitigate their tendency to become overloaded when other lines are removed. Phrased another way, the technique identifies lines whose low reactance predisposes them to creating binding security constraints in $(N-1)$ contingency scenarios. The problem of adding fixed reactances to lines in the grid is modelled as a mixed integer optimization problem.

To conclude, the major contributions of the present paper are summarised as follows:

- Using the grid's LODF matrix, a novel measure, termed median shadow capacity, is formulated to assess the loadability of a particular line of a power grid under all possible operational snapshots while imposing $(N-1)$ security constraints. This new metric revealed, as a very important insight into one of the leading causes of the $(N-1)$ congestion, that imbalances in the reactance structure of a power grid are significant.
- Using the results of the shadow capacity analysis, a novel congestion relief mechanism is developed that addresses the imbalances in the reactance structure of a power grid by adding fixed reactances to particular identified lines. By modifying the grid's reactance structure, the technique aims to avoid poor power flow re-distributions following a line outage, hence mitigating prospective overloading after an outage. In this manner, the burden of $(N-1)$ congestion is intended to be reduced.

Furthermore, screening and comparative analyses are conducted to examine the capabilities of the proposed congestion relief technique. To this end, firstly, using numerous operational snapshots created by a Monte Carlo methodology it is shown that the proposed strategy can modestly relieve $(N-1)$ congestion in many cases (an operational snapshot here refers to a specific generation-demand profile for the grid). While the achieved results are only modest, this application example does validate that the shadow capacity paradigm offers potentially useful insights on the structural origins of $(N-1)$ congestion in power grids. As a further step in evaluating and analyzing the proposed congestion relief, a comparison is carried out between the shadow capacity-based congestion relief scheme and a conventional generator re-dispatch approach. The integration of Renewable Energy Sources (RES) into modern power grids is substantial and escalating, resulting in an increase in generation dispatch uncertainty. Because of this, grids may be exposed to unanticipated generation dispatches that do not necessarily satisfy the $(N-1)$ security constraints. Under such scenarios, it is necessary for operators to re-dispatch the generators to satisfy the $(N-1)$ security constraints. In this paper, a generator re-dispatching technique is described as a typical congestion relief strategy, and its implementation outcomes are compared to those of the novel congestion relief strategy based on shadow capacity analysis.

The rest of the paper is organised as follows: In Section. III, the shadow capacity analysis and the novel $(N-1)$ congestion relief strategy are presented. Section. V provided the results obtained from implementing the proposed methodologies. Section. VI concludes.

II. Shadow Capacity

Consider the notional power grid in Fig. 1. This small network has the topology of a Wheatstone bridge: see [33] for a fuller discussion of how individual lines contribute to both reliability and congestion in such networks segments. The **pre-outage power flow** shows that line $A \to C$ transmits 272.73 MW and the other lines are working within their thermal limits also. If line $A \to C$ is tripped off, its **post-outage power flow** will evenly redistribute between two alternative paths of equal total reactance, $A \to B \to C$ and $A \to D \to C$. This power flow redistribution increases the power flow of line $B \to C$ to 150 MW, which is beyond its thermal capacity of 80 MVA and consequently, $B \to C$ would then be tripped off as well. Line outage security constraints exist to prevent circumstances like this arising [7], and would disallow this 300 MW transaction, likely requiring a more expensive generator dispatch to work around this $(N-1)$ congestion [6], [7], [34]. Note that the term *shadow* for the novel metric is chosen as an allusion to the *shadow price* of these $(N-1)$ security constraints.

Due to the reactance structure of Fig. 1, its LODF matrix would show that 50% of any flow along line $A \to C$ will redistribute to line $B \to C$ in the event of an outage. Assuming zero pre-outage power flow on line $B \to C$, the maximum allowable loading, termed *median shadow capacity*, of line $A \to C$ is therefore just 160 MW, as an outage at this loading level would redistribute 80 MW to line $B \to C$. This zero pre-outage flow assumption neither amplifies nor ameliorates line $B \to C$'s tendency to exceed its thermal limits. For this reason, this metric is deemed the *median* shadow capacity. Consider also the theoretically least-constraining scenario for Fig. 1, if a full 80 MW was somehow initially flowing in the direction $C \to B$, opposing the prospective redistributed power from the

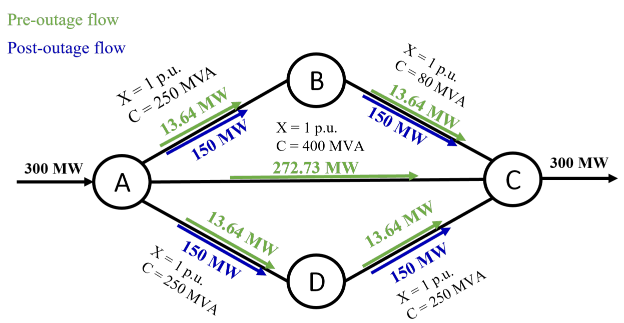

Fig. 1. An example power transaction from node A to C: in the **post-outage** situation, the power divides evenly between the upper and lower paths due to their equal total reactance, even though the capacity bottleneck at $B \to C$ cannot accommodate such a large share of the redistributed power

outage $A \to C$. This effectively doubles the available thermal capacity of $B \to C$. However, even this best-case effective capacity of 160 MW for of $B \to C$ would still impose a capacity limitation of 320 MW onto $A \to C$, which is still less than its physical limit of 400 MVA. Note that in practice, line outages usually increase parallel flows.

The restrictive shadow capacity of $A \to C$ stems from the *overly low* reactance of $B \to C$, which gives it a prominence in the LODF matrix that is disproportionate with its thermal capacity. For example, increasing the impedance of $B \to C$ to 4.52 $p.u.$ eliminates the reactance imbalance, so that the outage $A \to C$ would only transfer 79.89 MW onto $B \to C$, maintaining it within its limits. Likewise, the capacity of $B \to C$ could also be uprated to remediate this situation, though this would likely be more costly. Notably, in practice, lines with lower reactance have a higher loading capacity, and we have used this notional example grid to exemplify how the reactance structure of a power grid might affect its loadability. Note that adding more fixed reactances to specified lines does not directly affect their thermal capacity; rather, it tends to reduce the magnitude of power flows arising on such lines, and globally alters the loadability pattern of the grid. Several variables, including the conductor's structure, location, age, and the time of year, influence the thermal capacity of a transmission line [35]. In practice, there are several types of equipment that can be used to add extra fixed reactance to a particular line. For example, Distributed Series Reactances (DSR) [36], [37] can be implemented to add extra reactances to a line.

A. (N - 1) congestion relief

Based on the toy problem discussed above, it could be argued that shadow capacity limitations, and consequently the burden of $(N-1)$ congestion, are caused by imbalances between the reactance structure of a power grid and the capacities of particular lines. As a result, it can be conjectured that modifying the grid's reactance structure by deploying extra reactances could ease the unbalanced flow redistribution and, as a result, improve the lines' shadow capacities and relieve the $(N-1)$ congestion.

Thus, the $(N-1)$ congestion relief strategy articulated in the present paper is based on the proposed median shadow capacity analysis. The suggested strategy aims to improve the lines' shadow capacities, as much as it is possible, by deploying extra fixed reactance modules to be installed on particular identified lines. Importantly, it is argued that improving the median shadow capacities could result in reducing the $(N-1)$ congestion and consequently, improving the grid's overall loadabilty. In this way, cheaper generation schedules may be possible. Installing the extra fixed reactances is implemented to modify the grid's reactance structure.

III. Methodology

In this section, firstly, a novel methodology to assess the loadability of a particular line (under all operational snapshots for a power grid while imposing the line outage security constraint) by calculating median shadow capacities is proposed. Thereafter, a novel $(N-1)$ congestion relief strategy is articulated.

A. Calculation of Line Shadow Capacity

To calculate the LODF, first we obtain the Power Transfer Distribution Factor matrix, Π [32]. Under DC power flow approximations, the flow change in line l, connecting node i to node j, due to the injection of Λ MW at bus s and withdrawal at bus t, ${\Pi_l}^{st}$, is calculated as follows [32]:

$$ {\Pi_l}^{st} = \frac{\Theta_l^{st}}{\Lambda^{st}} \tag{1} $$

Where Θ_l^{st} is the shift in power on line l for an injection of Λ MW at bus s and withdrawal it at bus t. Considering the DC-PF assumptions, one could likewise calculate the changes in the buses' voltage angles as follows:

$$ \Delta\delta = Z_{bus} \times \Delta P \tag{2} $$

For injecting 1 MW of power at bus s and withdrawing it at bus t, i.e., $\Lambda^{st} = 1$ MW, the components at rows s and t of ΔP are 1 and -1, respectively, whereas the remaining components are 0, and consequently, from Equation (2), the voltage angle changes for buses i and j are calculated as follows:

$$ \begin{aligned} \Delta\delta_i &= x_{is} - x_{it} \\ \Delta\delta_j &= x_{js} - x_{jt} \end{aligned} \tag{3} $$

Where x_{is} is the imaginary part of the component at row i and column s within the grid's impedance matrix, Z_{bus}, the inverse of the admittance matrix, Y_{bus}. On the other hand:

$$ \Theta_l^{st} = \frac{(\Delta\delta_i - \Delta\delta j)}{X_l} \tag{4} $$

Where X_l is the reactance of line l. Replacing Equation (3) in Equation (4) gives:

$$ \Theta_l^{st} = \frac{(x_{is} - x_{it}) - (x_{js} - x_{jt})}{X_l} \tag{5} $$

Therefore, [32] establishes that the flow change in line l, connecting node i to node j, due to the injection of 1 MW at bus s and withdrawal at bus t, ${\Pi_l}^{st}$, is calculated as follow

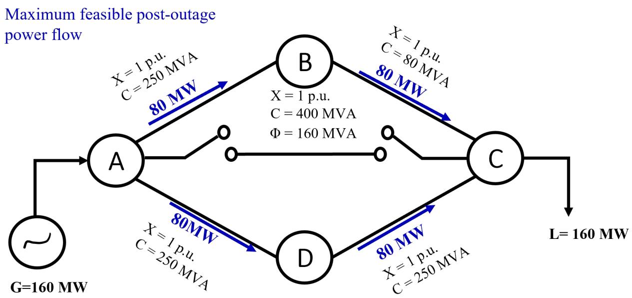

(a) Before adding the extra fixed reactances, the maximum feasible **power flow** from A to C is 160 MW, which loads the line $B \rightarrow C$ to its limit of 80 MVA

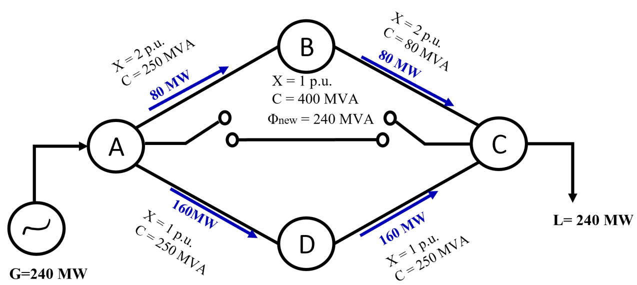

(b) After adding the extra fixed reactances the injection G and withdrawl L can be brought to a value of 240 MW before congestion occurs at $B \rightarrow C$

Fig. 2. A notional example to show how the power transaction from A to C can be modelled with a fictitious paired generator and load. Adding reactances to the upper path allows the magnitude of this transaction to be maximised to a higher value: this is exactly equivalent to increasing the shadow capacity of $A \rightarrow C$

$$\Pi_l{}^{st} = \frac{(x_{is} - x_{it}) - (x_{js} - x_{jt})}{X_l} \tag{6}$$

Using Equation (6) all the components of Π matrix are obtained in turn. Notably, the LODF approach depends on linearizing assumptions. As the scope of the present paper is to investigate the fundamental cause of $(N-1)$ congestion, these assumptions are appropriate, as they emphasise the dominant role played by line reactances and network structure in determining patterns of power flow redistribution. In practice, other factors, such as reactive power flows, will also be relevant to line loadability assessments, but these are excluded here to focus on the more fundamental causes.

For a line k outage, connecting nodes m and n, it is proven in [32] that the corresponding component of l within LODF matrix, $\Psi_l{}^k$, is obtained as follows:

$$\Psi_l{}^k = \frac{\Pi_l{}^{mn}}{1 - \Pi_k{}^{mn}} \tag{7}$$

Equation (7) describes what percentage of the flow in line k will be redistributed onto line l after outaging line k.

Let L' be the set of all the grid's lines except k. The median shadow capacity for k is defined as the maximum loading level of k for which its removal does not lead to any overloading in L'. We use the LODF to calculate the vector of loading levels, S, for a line k such that its removal would load each of the other lines within L' to their respective thermal capacities:

$$S_k = \{\frac{C_l}{\Psi_l{}^k}, \ \forall l \in L'\} \tag{8}$$

Where C_l is the thermal capacity of l. The minimum of S_k is the figure of interest: this is the specific loading level of k which ensures that redistribution of the line's flow after its removal will not overload any another line. Therefore, the median shadow capacity for k, Φ_k, is calculated by extracting the minimum value from the vector S_k:

$$\Phi_k = min \ \{S_k\} \tag{9}$$

We term the specific line in L' whose LODF participation causes the median shadow capacity restriction of k to be k's *constraining line*.

Line k can be categorised as follows:

$$\begin{cases} \textit{Unshadowed line} & \text{iff} \quad \Phi_k \geq C_k \\ \textit{Shadowed line} & \text{iff} \quad \frac{C_k}{2} \leq \Phi_k < C_k \\ \textit{Fully-constrained line} & \text{iff} \quad 0 \leq \Phi_k < \frac{C_k}{2} \end{cases} \tag{10}$$

This line categorisation is based on the theoretical *best* and *worst* loading scenarios for power redistribution. In the best loading scenario, the pre-contingency power flow on the constraining line is maximal and in the *opposite* direction to the redistributed power flow. This would act to double the constraining line's effective thermal capacity, in turn doubling the apparent shadow capacity of the constrained line. In the worst loading scenario, a constraining line would have maximal flow in the *same* direction as the redistributed power flow, leaving no remaining capacity and bringing the apparent shadow capacity of the constrained line to zero. The assumption of zero pre-outage power flow on the lines in L' is a midpoint between these extremes, and hence is termed the median shadow capacity. It should be noted that in practice these theoretical *best* and *worst* loading scenarios are quite rare. Indeed, the best and worst loading scenarios analysis based on the median shadow capacity metric provides a range of potential actual loading ampacity for a particular line for any generation dispatches of the grid when imposing the $(N-1)$ security constraints.

This analysis informs the categorisation in Equation (10): even in the best loading scenario, lines having $2\Phi_k < C_k$ will never be able to utilise their full thermal capacity, and are thus termed *fully-constrained*. Other lines having $\Phi_k < C_k$ appear to be in an unbalanced situation and at elevated risk of congestion in the $(N-1)$ sense, as they *require* a helpful pattern of pre-outage flows on adjacent lines to utilise their full thermal capacity. Note that even lines with $\Phi_k \geq C_k$ can still experience $(N-1)$ congestion, however this is only if they are *hindered* by flows in adjacent lines.

We define the *shadow bottleneck lines* to be those constraining lines that correspond to the shadowed or fully-constrained lines. The loading capacity decrease experienced by these constrained lines is calculated as:

$$\Delta_k = C_k - \Phi_k \tag{11}$$

Notably, the median shadow capacity analysis contributes significantly to the study of power grid loadability by: a) Determining a range of acheivable loading levels for the grid's lines while imposing the $(N-1)$ security constraints for any operational snapshots; b) Articulating the interactions between lines in terms of the congestion burden one line may impose on another (through identifying the *constrained* and *constraining* lines); and c) Identifying imbalances in the pattern of line reactances and thermal capacities are a key driver of the incidence of $(N-1)$ congestion.

B. Congestion Relief by Increasing Line Shadow Capacities

In this section, a novel strategy to relieve $(N-1)$ congestion is articulated. This strategy aims to improve the lines' median shadow capacities, which is hypothesised to make feasible and secure a wider breadth of potential generation schedules for a grid. This is because, according to Equation (10), the greater median shadow capacity a line has, the more likely it is to attain its maximum thermal capacity.

1) Modelling shadow capacity using fictitious paired loads and generators: Recall the notional grid shown in Fig. 1. It was observed that the shadow capacity of $A \rightarrow C$ was 160 MW, so that after $A \rightarrow C$'s removal no other line would be overloaded (with the assumption of zero pre-outage flow on other lines). The removal of $A \rightarrow C$ would necessitate that the power flow transaction of 160 MW would be facilitated by the rest of the grid. Fig 2 (a) shows such a post-outage power flow transactions across the grid of Fig. 1, with the removed line $A \rightarrow C$ here shown in a switched out state. As can be seen from this figure, the pre-outage flow of $A \rightarrow C$ can be modeled [38] as a fictitious injected generation (G) of 160 MW at bus A and a load (L) with the same magnitude at bus C. Therefore, the maximum feasible magnitude of the paired injected generation G at bus A and L at C is of interest as this describes the corresponding line's shadow capacity. This is an alternative approach to calculate, and optimize, the shadow capacities of lines within a grid.

An important observation is that we can modify the reactance structure of the grid so that higher G, L pairings become possible e.g improving the median shadow capacity of $A \rightarrow C$. We rely on this idea to articulate the novel strategy for improving the lines' shadow capacities and, hopefully, relieving the $(N-1)$ congestion. Among the available possibilities to modify the grid's reactance structure, one of the most applicable methodologies is simply to install fixed reactances on the identified lines. In the present paper, we rely on installing fixed reactances of one static rating to serve this purpose.

Consider Fig 2 (b) where lines $A \rightarrow B$ and $B \rightarrow C$ have been equipped with sufficient fixed reactances to increase their initial impedance from 1 P.U to 2 P.U. Following this modification in the grid's reactance structure, the transaction $G = 240$ MW becomes possible, which results in a median shadow capacity of 240 MW for $A \rightarrow C$. Hence, the intuition of adding reactance to a power grid to improve the lines' shadow capacity could be reasonable. Thus, the proposed strategy addresses the following question: where should fixed reactances be installed across the grid to achieve the highest rise in all G associated with the lines?

2) Optimization model of shadow capacity maximization: This problem is modeled as a Mixed Integer Linear Programming problem. For a grid with L lines and N buses, firstly, it is assumed line k is offline to calculate the shadow capacity of line k (connecting nodes m and n). Then, generator g_k, corresponding to line k, is connected to one side of the line (bus m) and, a load with the same size is connected to the other side (bus n). Note that these generators corresponding to the lines are fictional and are exploited to simulate their associated lines' median shadow capacities. The intuition is that by maximizing the fictional generation for a given line, the line's median shadow capacity is indeed aimed to be improved. Notably, calculating each line's shadow capacity using this methodology is a distinctive scenario, and therefore, the problem consists of L outage scenarios. Based on the DC power flow assumptions, the power flow on L_{ij} for maximising the k^{th} generation , P_{ij}^k, can be calculated as follow:

$$P_{ij}^k \times X_{ij}^{'} = \delta_i^k - \delta_j^k \quad |a_k = 0, \;\; k \neq L_{ij} \tag{12}$$

$$\sum_{(h \in N),\ (i \neq n,m)} P_{hi}^k = 0 \tag{13}$$

$$g_k + \sum_{(h \in N)} P_{hm}^k = 0 \tag{14}$$

$$-g_k + \sum_{(h \in N)} P_{hn}^k = 0 \tag{15}$$

$$\delta_s^k = 0 \tag{16}$$

where,

$$X_{ij}^{'} = X_{ij}^0 + U_{ij} \times X \tag{17}$$

Where X_{ij}^0 and X and $X_{ij}^{'}$ are the original natural reactance of L_{ij} and the fixed extra reactance added to L_{ij} and the new total reactance of L_{ij} all in P.U, respectively. U_{ij} is a binary decision variable so that $U_{ij} = 1$ if the line is equipped with the fixed extra reactance. Equations (13) to (15) impose the nodal injection constraints for this specific problem. Also, a_k denotes the status of line k and $a_k = 0$ means line k is offline and δ_i is the voltage angle of bus i. Importantly, in this problem, we aim to identify which lines are the optimal places for the fixed reactance units across all outage scenarios. Hence, the calculated U for all of the outage scenarios should be consistent. Equation (12) can be rewritten as follow:

$$P_{ij}^k \times (X_{ij}^0 + U_{ij} \times X) = \delta_i^k - \delta_j^k \tag{18}$$

$$P_{ij}^k \times X_{ij}^0 + P_{ij}^k \times U_{ij} \times X = \delta_i^k - \delta_j^k \tag{19}$$

Terms $P_{ij}^k \times U_{ij}$ of the problem are non-linear terms that can be substituted with another continuous variables, γ_{ij}^k, so that the following linear constraints based on *Big M* methodology [36], [39] must be met:

$$P_{ij}^k \times X_{ij}^0 + \gamma_{ij}^k \times X = \delta_i - \delta_j \tag{20}$$

$$P_{ij}^k - (1 - U_{ij}) \times M_{ij} \leqslant \gamma_{ij}^k \tag{21}$$

$$\gamma_{ij}^k \leqslant P_{ij}^k + (1 - U_{ij}) \times M_{ij} \tag{22}$$

$$\gamma_{ij}^k \leqslant U_{ij} \times M_{ij} \tag{23}$$

$$\gamma_{ij}^k \geqslant -U_{ij} \times M_{ij} \tag{24}$$

where M_{ij} is a sufficiently big and positive number. To avoid numerical issues once solving the problem, each M is proportional to its corresponding line's capacity [36]. All of the constraints stated in Equations (12) to (24) will be imposed for all ($g_k \in G$) simultaneously in order to determine all U_{ij}, thereby identifying the lines to be equipped with extra fixed reactances. Consequently, the problem of adding fixed reactances to improve the lines' shadow capacities is modeled as follows:

$$\text{Objective Function} = max(\sum_{g_k \in G} g_k) \tag{25}$$

S.t.:

(12) to (24)

$$-\eta_{ij} \leqslant P_{ij}^k \leqslant \eta_{ij}, \quad P_{ij}^k = 0 \ \ |k = L_{ij} \tag{26}$$

$$\forall k \in \hat{L} \tag{27}$$

where η_{ij} is the loading capacity of line L_{ij} and G is the set of all the added generators to the lines.

C. Validating Level of Congestion Relief

1) Creating numerous generation schedules: To explore the effects of adding the fixed reactances on $(N-1)$ congestion relief and consequently, improving a grid's loadability, numerous operational snapshots for the grid should be trialled before and after installing the modules. In this paper, we rely on a Monte Carlo methodology [40] to generate a sizeable number of generation schedules for the grid. To this end, for each operational snapshot, a random group of the generators is selected to be online. Notably, one may set the percentage of the active generators (μ) beforehand to a desirable value. The rest of the generators stay offline. Then, each of the online generators should randomly generate a level of active power within its corresponding permitted lower and upper generation bounds. Finally, spot loads within the grid are linearly scaled to the level of the grid's total generation.

2) Screening generation schedules for security: This section details the approach for determining the *feasibility* of each generation schedule created using the methods described in Section. III-C1. Here, a created generation schedule for a power grid is regarded *feasible* if the grid's operation, under that particular generation/demand profile and taking into account the DC-PF assumptions, satisfies the $(N-1)$ security constraints. This implies that, for a feasible dispatch, the DC-PF must be converged when the $(N-1)$ security constraints are imposed. All other generation schedules that do not meet this criterion are deemed *infeasible* and are considered to be insecure. This specific feasibility analysis can be performed for a case study before and after the installation of additional fixed reactances in order to evaluate the effects of these devices on alleviating the $(N-1)$ grid congestion.

D. Comparison Analysis

This section provides an analysis based on a typical strategy implemented by convectional methodologies to alleviate congestion, including $(N-1)$ congestion, so that the results of the novel shadow capacity-based alleviation strategy may be compared to those of the conventional techniques. Generation re-dispatching is one of the most effective conventional strategies for relieving congestion and the available approaches in the literature rely on it whole or in part [28], [41]. Importantly, altering generation for a given dispatch present both operational challenges and re-dispatching costs, as more expensive generation must be relied upon to avoid the congestion issue. Consequently, the analysis presented in this section seeks to re-dispatch an initially infeasible generation dispatch with the smallest generation disturbance (up- or down-regulation) for each generator, so that the new dispatch meets the $(N-1)$ security constraints. This problem is modelled as follows:

$$\text{Objective Function} = min(\sum_{\mathcal{G}_h \in \mathbb{G}} |\mathcal{G}_h - \mathcal{G}_h^0|) \tag{28}$$

S.t.:

$$P_{ij} \times X_{ij} = \delta_i - \delta_j \tag{29}$$

$$-\eta_{ij} \leqslant P_{ij} \leqslant \eta_{ij} \tag{30}$$

$$\sum_{\mathcal{G}_i \in \mathbb{G}_i} \mathcal{G}_i - D_i + \sum_{n \in N} P_{ni} = 0 \tag{31}$$

$$\delta_s = 0 \tag{32}$$

$$P_{ij}^k \times X_{ij} = \delta_i^k - \delta_j^k \quad |a_k = 0, \ \ k \neq L_{ij} \tag{33}$$

$$-\eta_{ij} \leqslant P_{ij}^k \leqslant \eta_{ij}, \quad P_{ij}^k = 0 \ \ |k = L_{ij} \tag{34}$$

$$\sum_{\mathcal{G}_i \in \mathbb{G}_i} \mathcal{G}_i - D_i + \sum_{n \in N} P_{ni}^k = 0 \tag{35}$$

$$\mathcal{G}_h^{min} \leq \mathcal{G}_h \leq \mathcal{G}_h^{max} \tag{36}$$

$$\delta_s^k = 0 \tag{37}$$

The objective function presented in Equation (28) seeks the minimum generation redispatch for each generator. Also, note that Equations (33) to (37) impose the $(N-1)$ security constraints and will be applied to $(\forall\ k \in \hat{L}\ )$.

For each generator, the minimum generation change achieved from the aforementioned analysis is defined as the generator's *generation disturbance*.

$$\Delta\mathcal{G}_h = \mathcal{G}_h - \mathcal{G}_h^0 \tag{38}$$

We define the set of all generation disturbances for the generators as *generation disturbances set*:

$$\Delta\mathbb{G} = \{\Delta\mathcal{G}_h,\ \forall\mathcal{G}_h \in \mathbb{G}\} \tag{39}$$

IV. Test Platform

Three sample grids (small, medium and large) from the repository at [35] are selected to evaluate the suggested methodology. These sample grids are: `pglib_opf_case39_epri`, `pglib_opf_case588_sdet`, and `pglib_opf_case2383wp_k`. The original thermal limits for the lines within `pglib_opf_case39_epri` have been reported in [42]. `pglib_opf_case588_sdet` is a synthetic sample grid developed by Sustainable Data Evolution Technology (SDET) [43] and the thermal limits for the lines are those reported by the SDET. This study includes the sample grids `pglib_opf_case2383wp_k` and `pglib_opf_case39_epri` to assess the proposed techniques using real power grids. `pglib_opf_case2383wp_k` is the Polish transmission network and the thermal capacities of the lines are realistic thermal capacity that have been reported in [44], [45]. Also, `pglib_opf_case39_epri` represents the New England 345 KV network [44]. Radial lines are not included in the shadow capacity calculations since removing a radial line does not overload another line within the grids. MATPOWER [44] is used to perform the calculations. The optimisation problem of adding the reactances to the grids is handled by YALMIP [46] toolbox on MATLAB [47]. The simulations scripts and resulting data can be found in a persistent online repository at [48].

A. Practical Challenges in Estimating Line Loading Capacities

Loading capacity for the lines of a high voltage transmission system can be restricted by different operative factors like thermal capacity, voltage and stability limits [49]. There are generally considerable challenges for all academic researchers in the field to access appropriate data on line limits. To tackle this challenge, the loading capacity for the lines can be estimated by the techniques like the ones proposed in [35]. A major concern related to such estimations is that they could be very approximate, so that lines may not be coordinated. Due to these concerns, the thermal limit is selected as a proxy for the loading capacity in the presented paper. Notably, as discussed in [50], using thermal limits to define lines' loading capacity usually applies to lower voltage transmission systems with lines less than 80 KM in length. Thus, for realistic grids that meet these conditions the thermal capacity can be selected reasonably to bind the lines' loading capacities. Obviously, one may opt for the other line loading limits as a proxy for the loading capacity and implement the proposed methodology in case of having accessing to more realistic loading capacity parameters.

TABLE I. Categorisation of line types

Test network	# All lines	# Radial lines	# Un-shadowed	# Shad-owed	# Fully-constrained
case39_epri	46	11	20	15	0
case588_sdet	686	235	146	197	108
case2383wp_k	2894	642	918	1214	120

V. Results

A. Shadow Capacity Analysis

The scatterplots in Fig. 3 compare the median shadow capacities Φ_k and thermal capacities C_k for the lines within the sample grids. The areas between the two black lines in this figure show the shadowed lines. Such lines appear unbalanced in some sense, as operating them at their full capacities requires compensatory flows on adjacent lines. Also, Fig. 4 visualises [51] the identified lines within the three sample networks corresponding to Fig. 3.

Fig. 3 also shows, in red, a considerable number of fully-constrained lines in panes (b) and (c). No fully-constrained lines are reported for `pglib_opf_case39_epri`. Such lines can never reach their thermal capacities under any operational snapshots. The shadow capacities analysis implies that these networks are suffering from unbalanced development patterns and seem prone to congestion, as many of their lines are precluded from using their available thermal capacities.

Table. I also shows that there are lines within all three grids with shadow capacities less than their corresponding thermal capacities. The distributions of the capacity decreases Δ_k suffered by these lines are shown in Fig. 5. 2.5%, 37.1% and 17% decreases in the loading capacities of the shadowed and fully-constrained lines are reported for `pglib_opf_case39_epri`, `nesta_case588_sdet`, and `nesta_case2383wp_k`, respectively. This indicates that the shadow capacities of some lines within the grids are quite restrictive, and this raises questions on why such lines were specified with such high ampacities that they are precluded from using by the reactance and capacities of adjacent lines.

The histograms in Fig. 6 display the *aggregate* loading capacity decrease attributable to each bottleneck line (note that a particular line can act as a bottleneck for several constrained lines) From Fig. 6, one can note that the worst bottleneck lines, at the left of each pane, can cause a very significant loss of aggregate transmission capacity, up to 3.8 GW in certain cases. These critical shadow bottleneck lines are therefore a key originator of $(N-1)$ congestion.

These critical bottleneck lines could be targeted for capacity uprating to optimize the holistic network structure. Alternatively, adding fixed reactance to such bottlenecks may reduce their LODF participation and thus ameliorate their tendency to cause $(N-1)$ congestion. Fundamentally, it is the lack

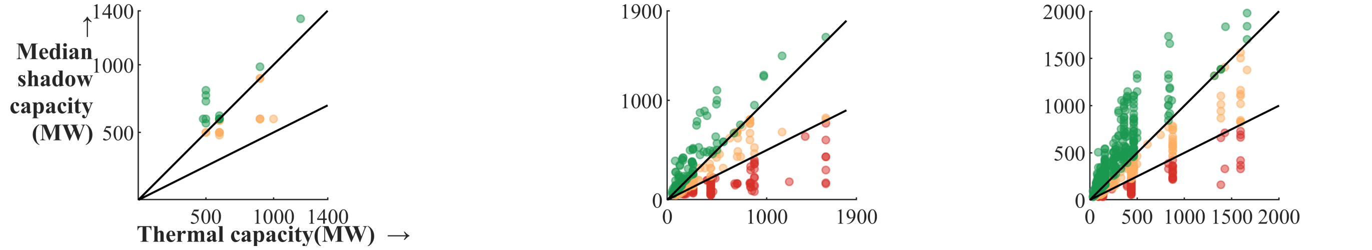

(a) pglib_opf_case39_epri (b) pglib_opf_case588_sdet (c) pglib_opf_case2383wp_k

Fig. 3. Shadow and thermal capacities comparison. Points in green denote **unshadowed lines**, in orange **shadowed lines** and in red **fully-constrained lines**

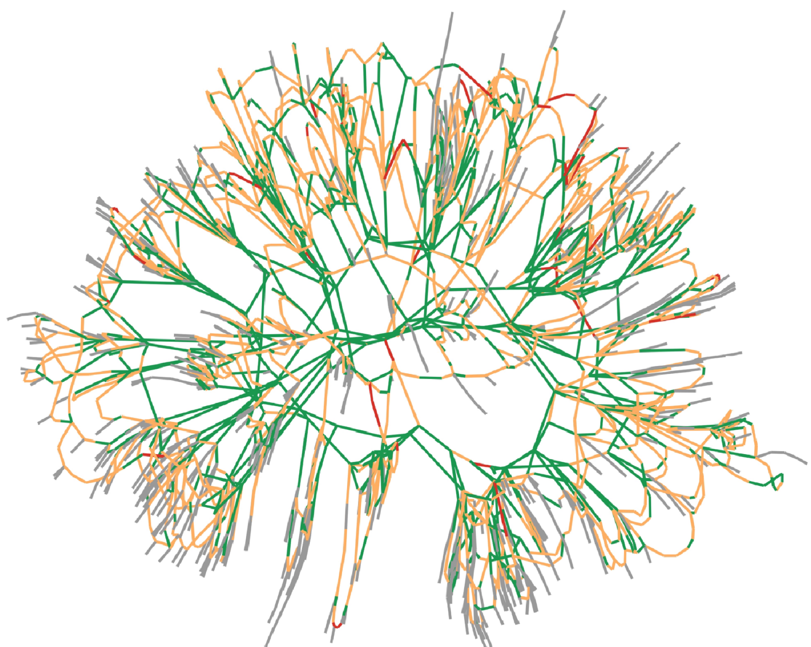

(c) pglib_opf_case2383wp_k

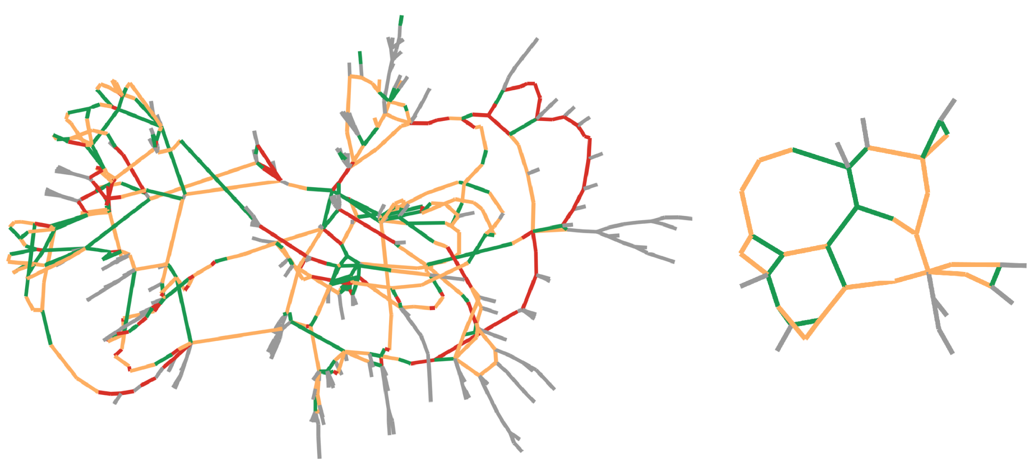

(b) pglib_opf_case588_sdet (a) pglib_opf_case39_epri

Fig. 4. Descriptive visualisation for the three sample grids. Lines in green denote **unshadowed lines**, in orange **shadowed lines** and in red **fully-constrained lines**

of harmony between the reactance, capacity, and location of these bottleneck lines that causes the congestion elsewhere. Indeed, the various existing optimal transmission switching methodologies [13]–[16] could be viewed in this light, as removing a line increases its reactance to infinity.

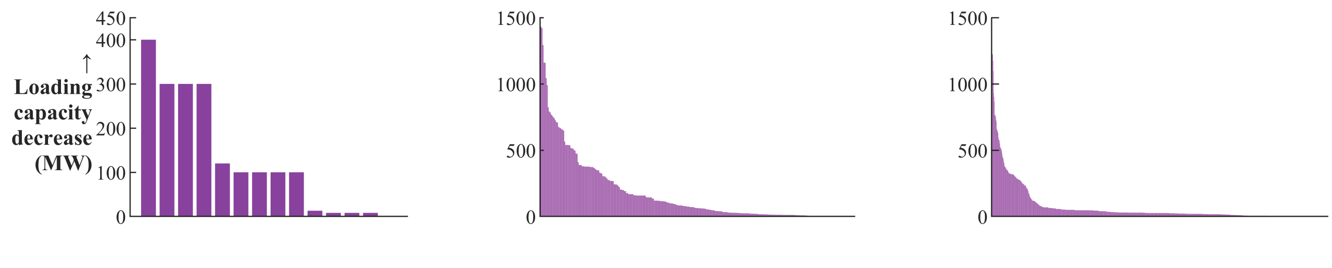

(a) `pglib_opf_case39_epri` (b) `pglib_opf_case588_sdet` (c) `pglib_opf_case2383wp_k`

Fig. 5. Loading capacity decrease (Δ_k) experienced by each affected line k, sorted in descending order with each bar representing a distinct line

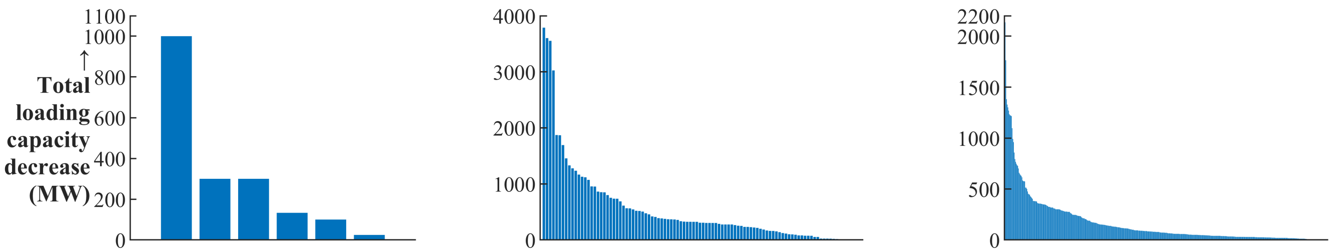

(a) `pglib_opf_case39_epri` (b) `pglib_opf_case588_sdet` (c) `pglib_opf_case2383wp_k`

Fig. 6. The total loading decrease attributable to each specific bottleneck line ($\sum \Delta_k$), sorted in descending order with each bar representing a distinct line

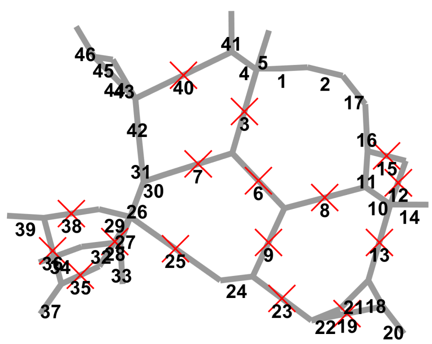

Fig. 7. Descriptive visualization for `pglib_opf_case39_epri`, the lines marked with X are the identified lines to install the extra fixed reactances by the proposed methodology. Each line's number can also be seen

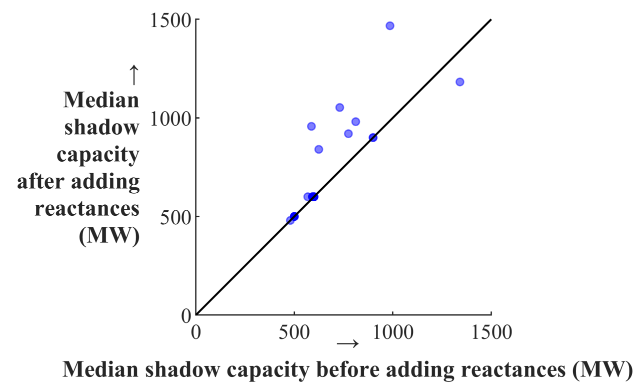

Fig. 8. A comparison between the lines' median shadow capacities before and after adding the fixed reactances for `pglib_opf_case39_epri`

TABLE II. Feasibility screening of `pglib_opf_case39_epri` Monte Carlo generation schedules

	Few generators $\mu \leq 30\%$	Some generators $30\% < \mu \leq 90\%$	Many generators $\mu > 90\%$	
Created schedules	3000	3000	4000	$\sum$ = 10000
Feasible before	2157	824	417	$\sum$ = 3398
Feasible after	2270	1020	670	$\sum$ = 3960
Infeasible → feasible	114	198	254	$\sum$ = 566
Feasible → infeasible	1	2	1	$\sum$ = 4

B. Congestion Relief

As a further extension of the shadow capacity analysis of power systems, the congestion alleviation optimisation technique from Section III. B. is applied to the smaller of the three test networks, `pglib_opf_case39_epri`. The modest size of this network mitigates the computational demands of implementing the optimization. To evaluate the performance of the suggested technique, we simply, and arbitrarily, suppose that discrete fixed reactances can add 0.1 p.u. to their corresponding lines' reactances.

1) Siting the extra reactances: Fig. 7 visualises `pglib_opf_case39_epri` and shows the lines identified by the optimisation methodology as apt locations to install the fixed extra reactances. Of the 46 lines in the network, 16 are identified as the optimal places to install the fixed reactance modules.

Firstly, the effects of these additional reactances on the lines' shadow capacities are investigated. Fig. 8 compares the shadow capacities of the lines within `pglib_opf_case39_epri` before and after installing the reactances. From this figure, one

TABLE III. Generation disturbance screening of `pglib_opf_case39_epri` for infeasible Monte Carlo generation schedules

		Few generators $\mu \leq 30\%$	Some generators $30\% < \mu \leq 90\%$	Many generators $\mu > 90\%$	For all μ
Unsavable schedules	Number of schedules	729	1978	3329	$\sum = 6036$
	$\lvert\Delta\mathbb{G}\rvert_{Av}$	315.9 MW	560.7 MW	702.8 MW	609.5 MW
	$\lvert\Delta\mathbb{G}\rvert_{max}$	1575.6 MW	2424.6 MW	5865.2 MW	5865.2 MW
	$\lvert\Delta\mathbb{G}\rvert_{min}$	0.3 MW	0.1 MW	0.7 MW	0.1 MW
Savable schedules	Number of schedules	114	198	254	$\sum = 566$
	$\lvert\Delta\mathbb{G}\rvert_{Av}$	194.9 MW	187.7 MW	213.4 MW	200.7 MW
	$\lvert\Delta\mathbb{G}\rvert_{max}$	534.3 MW	567.7 MW	570.8 MW	570.8 MW
	$\lvert\Delta\mathbb{G}\rvert_{min}$	3.2 MW	1 MW	0.7 MW	0.7 MW

can notice that the median shadow capacities of the lines, except for one line, are equal or greater than their initial values. Therefore, it is conjectured that under this new condition the grid faces less congestion corresponding to the line outage security constraints, and consequently, more potential generation schedules become feasible.

To evaluate the implications of these median shadow capacity improvements on the overall grid's loadability, the grid should be evaluated before and after installing the extra reactances for the generation schedules created using the Monte Carlo strategy.

2) Feasibility screening assessment for potential generation schedules: To explore if adding the reactances to `pglib_opf_case39_epri` is effective at relieving the $(N-1)$ congestion and thus enabling a greater number of potential generation schedules that satisfy the line outage security constraints, in this section, $10,000$ generation schedules are created for the grid's generation units using a Monte Carlo methodology. To ensure the sampling covers a range of grid operational conditions, we deliberately create schedules with different percentage bands for number of units online, to represent regimes with *few*, *some*, and *many* active generators.

After creating the random generation schedules using the Monte Carlo methodology, we investigate if each of them meets $(N-1)$ security constraints before and after adding the reactances. To this end, we rely on the conventional DC power flow as a screening tool: if removing any line under a particular random generation schedule causes overloading elsewhere, that schedule can be deemed *infeasible*. The details of this analysis can be found in Table. III.

The data in Table. III demonstrates that, prior to adding reactances, only 3398 out of $10,000$ created schedules satisfy the $(N-1)$ security constraints. Following the addition of the reactances, 3960 out of $10,000$ created schedules meet the $(N-1)$ security constraints, meaning that the additional reactances made an additional 562 $(N-1)$ dispatch schedules feasible, an increase of 16.5%. Such improvements are evident across all three generation regimes. In certain rare cases, schedules that were initially secure were made insecure by the addition of the reactances; just four incidents of such reversion were noted.

Overall, the results in Table. III demonstrate that the proposed optimization methodology successfully reduced the incidence of $(N-1)$ congestion for the grid by adding fixed reactances that target shadow capacity maximiszation. This expanded the space of feasible generation schedules by 16.5%.

3) Comparative analysis using a generation re-dispatch congestion relief strategy: This section compares the efficacy of deploying fixed reactances against employing a conventional congestion relief strategy based on re-dispatching generation. The methodology for this remedial generation redispatch was presented in Section III-D.

The results of this analysis can be found in Table III. This table focuses on the generation dispatch snapshots that were initially infeasible but then became feasible by installing the fixed reactances. Accordingly, we divide the originally infeasible generation schedules into two categories: *savable schedules* are infeasible dispatches that can be rendered feasible by installing extra fixed reactances, whereas *unsavable schedules* are infeasible dispatches that cannot be made feasible by reactance installations. The re-dispatching strategy ensures minimal *generation disturbances* for each generator in order to achieve operational feasibility for an initially infeasible snapshot. The results in Table III show that significant disturbance of the desired generation schedules for all μ would be required to achieve $(N-1)$ feasibility in the initially infeasible cases. The reported averages of the total generation disturbances are roughly greater than 200 MW for the savable schedules, indicating, on average, 10.4% of the total generation for the savable schedules must be re-dispatched (The average of total generation for the savable schedules is reported 1939.4 MW). This is a sizeable amount of generation disturbance that should be conducted to make the savable generation schedules feasible using the re-dispatching technique.

It should be noted that altering the generation profiles incurs operational complications and additional costs for the grid's operation. Considering this critical point in conjunction with fairly large required generation disturbances reported in Table III suggests that the proposed method of alleviating the congestion by deploying fixed reactances seems a reasonable strategy for dealing with the congestion.

C. Discussion

In this section, some important points regarding the proposed methodologies are discussed.

1) Interpreting shadow capacity gains: First and foremost, while Fig. 8 shows that adding reactance may unlock additional shadow capacity for certain lines, the mapping of these shadow capacity gains to actual congestion reduction is complicated. While the Monte Carlo assessment and the comparison analysis indicated that additional reactances can be effective at alleviating $(N-1)$ security constraints, in realistic grids the desired generation schedules depend on likely fuel prices and the disposition of renewable sources. While this work has presented a validation of the underlying concept, in a more practical application it would be necessary to appraise the efficacy of the methodology in alleviating the actual sources of $(N-1)$ congestion for realistic generation schedules.

For these reasons, the actual gains in loading capacity for some grids may fall short of our expectations based on the results of the congestion alleviation strategy implementation. The results of earlier work in [36] shed light on this critical argument, indicating that adding additional impedance to the grid to prevent overloading following an outage may not be successful at preventing cascading failures. Thus, the results of implementing the proposed congestion-relief technique should be interpreted cautiously, since they are being used only as a proof-of-concept to provide additional context for the concept of shadow capacities. Additionally, more sophisticated optimization approaches may free up even more additional shadow capacity, making this an open research area for future studies.

2) Limitations of the optimization formulation: It should be noted that the provided formulation for adding reactances to the grids mentioned in Section. III-B can be further adapted to fit desired purposes. For example, no limits on the number of available lines for adding reactances were considered in the provided formulation. By setting the summation of the binary decision variables U to a desirable value this constraint can be imposed quite simply. Also, one may try to individually optimize the magnitudes of the added extra reactances to improve the results Additionally, in Fig. 8, it can be seen that one line's median shadow capacity has decreased slightly. This is because the objective function in Equation (25) maximizes the sum of all G. In such cases, the optimization may result in a solution where one or more lines are slightly worse off while the overall grid's total shadow capacities improve. To avoid such solutions, one might add a lower bound to the corresponding G for each line, requiring that the new shadow capacity be equal or greater than the line's initial shadow capacity. Moreover, if the objective function is set to increase the median shadow capacity of a particular line, a larger increase may be obtained for that line's median shadow capacity as the current objective function may be forced to conduct trade-off between all feasible potential locations for the raectances in order to increase the median shadow capacities of the lines overall. Another point is that, in this paper, we simply, and arbitrarily, set the magnitude of each extra reactance to be 0.1 $p.u.$ to initially explore the efficacy of the proposed methodology. In practice, one could set this value according to the real-world fixed reactances specifications.

3) Modern power grids' specifications and the proposed congestion alleviation technique: RES, such as solar power plants and wind farms, contribute significantly to the overall amount of generated power in modern power grids, and this contribution is expanding rapidly. As the output of such sources is dependent on uncertain external factors such as wind speed and solar radiation, their integration into the grid increases the uncertainty of generation dispatches and, as a result, may impose an unanticipated load-generation profile on the operation. Consequently, the conventional solutions for dealing with congestion that rely on re-dispatching the generations face notable challenges. That is, such techniques commonly encounter unexpected generation-load profiles that may not satisfy the $(N-1)$ security constraints, necessitating generation modification, which incurs substantial extra costs in power markets and exposes the grid to a variety of operation problems. In contrast, the strategy proposed in this paper does not rely on generation dispatches to alleviate congestion; rather, it focuses on one of the primary causes of congestion, namely imbalances in the reactance structure of the grid, and attempts to modify the impedance structure of the network to alleviate such congestion. This crucial aspect of the presented strategy is suggestive of its advantages over other conventional congestion management techniques, as the performance of the technique will not be impacted by unanticipated generation profiles as a result of the RES.

4) Computational complexity: Regarding the time complexity of the novel proposed congestion relief strategy, it is important to note that the technique is intended for planning studies for a power grid, implying that it is not intended to be implemented in real-time, and therefore, low time complexity and run-time are not essential and targeted. Despite the fact that the methodology is not expected to have a low computational complexity, the proposed formulation for the novel congestion relief strategy is convex and linear, resulting in a satisfactory computational complexity for the planning studies. The simulation of the proposed congestion technique for the case study was performed on a personal desktop computer with an Intel(R) Core(TM) i7 – 7700 processor and takes 403.2 seconds (about 6.5 minutes)to be converged.

VI. Conclusions

This paper investigated the structural determinants of power system $(N-1)$ congestion. To this end, a novel structural metric, termed median shadow capacity, was proposed, which assesses the usable capacity of lines in light of line outage security constraints elsewhere. The shadow capacities analysis was applied to three networks and revealed that, even for the best loading scenario, some lines, i.e., fully-constrained lines, can never operate at their rated thermal capacities. Based on the obtained results, this paper identified the reactance and topological structure of power grids as one of the fundamental causes of such congestion. On the basis of the insights gained during this step, a novel congestion relief technique based on the addition of fixed reactance modules to the identified lines was devised in order to increase the lines' median shadow capacity in general and consequently, alleviate the incidence of $(N-1)$ congestion. The problem of adding the fixed reactances to the grid was modeled as a new MILP problem. Implementing the technique successfully decreased the incidence of $(N-1)$ congestion: an additional 16.5% of the randomly created generation schedules become feasible and secure in the presence of the additional reactances. Such a widening of the feasible space should enable more cost-effective generation plans for grids. Further analyses were also undertaken to explore the potential capabilities of the suggested congestion strategy utilizing a comparison analysis based on a conventional generation redistribution technique. The findings of this analysis indicated that the proposed method of deploying fixed reactances can be considered as one of the reasonable strategies for addressing the congestion.

References

[1] M. Khanabadi, Y. Fu, and C. Liu, "Decentralized transmission line switching for congestion management of interconnected power systems," *IEEE Transactions on Power Systems*, vol. 33, no. 6, pp. 5902–5912, 2018.

[2] B. C. Lesieutre and J. H. Eto, "Electricity transmission congestion costs: A review of recent reports," Oct. 2003. [Online]. Available: https://www.osti.gov/biblio/821764.

[3] M. H. Haque, "Determination of steady-state voltage stability limit using P-Q curve," *IEEE Power Engineering Review*, vol. 22, no. 4, pp. 71–72, 2002.

[4] D. Pozo and J. Contreras, "A chance-constrained unit commitment with an N-k security criterion and significant wind generation," *IEEE Transactions on Power Systems*, vol. 28, no. 3, pp. 2842–2851, 2013.

[5] G. A. Orfanos, P. S. Georgilakis, and N. D. Hatziargyriou, "A more fair power flow based transmission cost allocation scheme considering maximum line loading for N-1 security," *IEEE Transactions on Power Systems*, vol. 28, no. 3, pp. 3344–3352, 2013.

[6] O. B. Tor, A. N. Guven, and M. Shahidehpour, "Congestion-driven transmission planning considering the impact of generator expansion," *IEEE Transactions on Power Systems*, vol. 23, no. 2, pp. 781–789, 2008.

[7] G. B. Shrestha and P. A. J. Fonseka, "Congestion-driven transmission expansion in competitive power markets," *IEEE Transactions on Power Systems*, vol. 19, no. 3, pp. 1658–1665, 2004.

[8] K. Tlijani, T. Guesmi, and H. Hadj Abdallah, "Optimal number, location and parameter setting of multiple TCSCs for security and system loadability enhancement," in *10th International Multi-Conferences on Systems, Signals Devices 2013 (SSD13)*, 2013, pp. 1–6.

[9] P. Malathy and A. Shunmugalatha, "Enhancement of maximum loadability during n-1 and n-2 contingencies with multi type facts devices and its optimization using mde algorithm," in *2016 IEEE UPCON*, 2016, pp. 173–178.

[10] S. Omran, R. Broadwater, J. Hambrick, M. Dilek, C. Thomas, and F. Kreikebaum, "Load growth and power flow control with dsrs: Balanced vs unbalanced transmission networks," *Electric Power Systems Research*, vol. 145, pp. 207–213, 2017.

[11] Y. Sang and M. Sahraei-Ardakani, "Effective power flow control via distributed facts considering future uncertainties," *Electric Power Systems Research*, vol. 168, pp. 127–136, 2019.

[12] Y. Sang and M. Sahraei-Ardakani, "The interdependence between transmission switching and variable-impedance series facts devices," *IEEE Transactions on Power Systems*, vol. 33, no. 3, pp. 2792–2803, 2018.

[13] E. B. Fisher, R. P. O'Neill, and M. C. Ferris, "Optimal transmission switching," *IEEE Transactions on Power Systems*, vol. 23, no. 3, pp. 1346–1355, 2008.

[14] M. Khanabadi, H. Ghasemi, and M. Doostizadeh, "Optimal transmission switching considering voltage security and n-1 contingency analysis," *IEEE Transactions on Power Systems*, vol. 28, no. 1, pp. 542–550, 2013.

[15] K. W. Hedman, M. C. Ferris, R. P. O'Neill, E. B. Fisher, and S. S. Oren, "Co-optimization of generation unit commitment and transmission switching with n-1 reliability," *IEEE Transactions on Power Systems*, vol. 25, no. 2, pp. 1052–1063, 2010.

[16] F. Pourahmadi, M. Jooshaki, and S. H. Hosseini, "A dynamic programming-based heuristic approach for optimal transmission switching problem with n-1 reliability criterion," in *2016 International Conference on PMAPS*, 2016, pp. 1–7.

[17] T. Altun, R. Madani, and A. Davoudi, "Topology-cognizant optimal power flow in multi-terminal dc grids," *IEEE Transactions on Power Systems*, vol. 36, no. 5, pp. 4588–4598, 2021.

[18] S. Fattahi, J. Lavaei, and A. Atamtürk, "A bound strengthening method for optimal transmission switching in power systems," *IEEE Transactions on Power Systems*, vol. 34, no. 1, pp. 280–291, 2019.

[19] W. E. Brown and E. Moreno-Centeno, "Transmission-line switching for load shed prevention via an accelerated linear programming approximation of ac power flows," *IEEE Transactions on Power Systems*, vol. 35, no. 4, pp. 2575–2585, 2020.

[20] R. S. Biswas, A. Pal, T. Werho, and V. Vittal, "A graph theoretic approach to power system vulnerability identification," *IEEE Transactions on Power Systems*, vol. 36, no. 2, pp. 923–935, 2021.

[21] ——, "Mitigation of saturated cut-sets during multiple outages to enhance power system security," *IEEE Transactions on Power Systems*, vol. 36, no. 6, pp. 5734–5745, 2021.

[22] A. Beiranvand and P. Cuffe, "A topological sorting approach to identify coherent cut-sets within power grids," *IEEE Transactions on Power Systems*, vol. 35, no. 1, pp. 721–730, 2020.

[23] H. Cetinay, F. A. Kuipers, and P. Van Mieghem, "A topological investigation of power flow," *IEEE Systems Journal*, vol. 12, no. 3, pp. 2524–2532, 2018.

[24] E. P. R. Coelho, M. H. M. Paiva, M. E. V. Segatto, and G. Caporossi, "A new approach for contingency analysis based on centrality measures," *IEEE Systems Journal*, vol. 13, no. 2, pp. 1915–1923, 2019.

[25] M. R. Narimani *et al.*, "Generalized contingency analysis based on graph theory and line outage distribution factor," *IEEE Systems Journal*, vol. 16, no. 1, pp. 626–636, 2022.

[26] K. Zheng, Q. Chen, Y. Wang, C. Kang, and L. Xie, "Unsupervised congestion status identification using lmp data," *IEEE Transactions on Smart Grid*, vol. 12, no. 1, pp. 726–736, 2021.

[27] C. Lo Prete, N. Guo, and U. V. Shanbhag, "Virtual bidding and financial transmission rights: An equilibrium model for cross-product manipulation in electricity markets," *IEEE Transactions on Power Systems*, vol. 34, no. 2, pp. 953–967, 2019.

[28] R. Chen, I. C. Paschalidis, M. C. Caramanis, and P. Andrianesis, "Learning from past bids to participate strategically in day-ahead electricity markets," *IEEE Transactions on Smart Grid*, vol. 10, no. 5, pp. 5794–5806, 2019.

[29] E. L. Miguelez *et al.*, "A practical approach to solve power system constraints with application to the Spanish electricity market," *IEEE Transactions on Power Systems*, vol. 19, no. 4, pp. 2029–2037, 2004.

[30] A. Hoffrichter, K. Kollenda, M. Schneider, and R. Puffer, "Simulation of curative congestion management in large-scale transmission grids," in *2019 54th UPEC*, 2019, pp. 1–6.

[31] Á. S. Xavier, F. Qiu, F. Wang, and P. R. Thimmapuram, "Transmission constraint filtering in large-scale security-constrained unit commitment," *IEEE Transactions on Power Systems*, vol. 34, no. 3, pp. 2457–2460, 2019.

[32] A. J. Wood, B. F. Wollenberg, and G. B. Sheblé, in *Power generation, operation, and control*, Wiley, 2014.

[33] S. Blumsack, L. B. Lave, and M. Ilic, "A quantitative analysis of the relationship between congestion and reliability in electric power networks," *The Energy Journal*, vol. 28, no. 4, 2007.

[34] M. Kristjónsson, "Enforcing the n-1 criterion in power transmission networks: An analysis of a theoretical model," M.S. thesis, Norwegian School of Economics, 2013.

[35] S. Babaeinejadsarookolaee *et al.*, "The power grid library for benchmarking ac optimal power flow algorithms," 2019. arXiv: 1908.02788 [math.OC].

[36] A. Beiranvand and P. Cuffe, "Negative results on deploying distributed series reactance devices to improve power system robustness against cascading failures," *IEEE Transactions on Power Systems*, vol. 36, no. 6, pp. 5210–5221, 2021.

[37] A. Soroudi, P. Maghouli, and A. Keane, "Resiliency oriented integration of dsrs in transmission networks," *IET Generation, Transmission Distribution*, vol. 11, no. 8, pp. 2013–2022, 2017.

[38] P. Cuffe and A. Keane, "A deterministic approach to locating series flow-controllers within transmission systems to alleviate congestion," *Electric Power Systems Research*, vol. 163, pp. 686–695, 2018, Advances in HV Transmission Systems.

[39] A. Nouri, S. H. Hosseini, and A. Keane, "Stochastic network constrained payment minimisation in electricity markets," English, *IET Generation, Transmission Distribution*, vol. 13, 2268–2279(11), 11 Jun. 2019.

[40] M. Mazumdar and L. Chrzan, "Monte Carlo stochastic simulation of electric power generation system production costs under time-dependent constraints," *Electric Power Systems Research*, vol. 35, no. 2, pp. 101–108, 1995.

[41] M. Panto, "Market-based congestion management in electric power systems with exploitation of aggregators," *International Journal of Electrical Power Energy Systems*, vol. 121, p. 106 101, 2020.

[42] "Transfer capability calculator," 2001. [Online]. Available: http://www.pserc.cornell.edu/tcc/.

[43] Z. Huang *et al.*, "Sustainable data evolution technology (SDET) for power grid optimization (final report)," Dec. 2018. [Online]. Available: https://www.osti.gov/biblio/1524091.

[44] R. D. Zimmerman, C. E. Murillo-Sánchez, and R. J. Thomas, "Matpower: Steady-state operations, planning, and analysis tools for power systems research and education," *IEEE Transactions on Power Systems*, vol. 26, no. 1, pp. 12–19, 2011.

[45] C. Coffrin, D. Gordon, and P. Scott, "NESTA, the NICTA energy system test case archive," 2014.

[46] J. Lofberg, "YALMIP : A toolbox for modeling and optimization in MATLAB," in *2004 IEEE International Conference on Robotics and Automation (IEEE Cat. No.04CH37508)*, Sep. 2004, pp. 284–289.

[47] MATLAB, *version 7.10.0 (R2019a)*. Natick, Massachusetts: The MathWorks Inc., 2019.

[48] A. Beiranvand and P. Cuffe, "Raw data and scripts from structural determinants of power system congestion," 2021. [Online]. Available: https : / / figshare . com / s / 031fdd019c6928fe2dd1.

[49] G. S. Bolacell and M. Augusto da Rosa, "Composite power system reliability assessment considering transmission line flexibility," in *2020 International Conference on PMAPS*, 2020, pp. 1–6.

[50] R. Gutman, P. Marchenko, and R. Dunlop, "Analytical development of loadability characteristics for EHV and UHV transmission lines," *IEEE Transactions on Power Apparatus and Systems*, vol. PAS-98, no. 2, pp. 606–617, 1979.

[51] P. Cuffe and A. Keane, "Visualizing the electrical structure of power systems," *IEEE Systems Journal*, 2015.